Kufa Journal of Engineering
Vol. 15, No. 3, July 2024, P.P. 1-20
Article history: Received 5 December 2023, last revised 9 February 2024, accepted 9 February 2024

BEHAVIOR OF REINFORCED CONCRETE CONTINUOUS DEEP BEAMS WITH OPENINGS AND USING MULTIPLE TYPES OF STRENGTHING

Huda Basim Ketab[1] and Muhammad Abed Attiya[2]

[1] MSc student, Civil Engineering, Department Faculty of Engineering, University of Kufa, Najaf, Iraq. Email: hudabasim1995@gmail.com

[2] Assistant Professor, Civil Engineering, Department Faculty of Engineering, University of Kufa, Najaf, Iraq. Email: mohammedw.alfatlawi@uokufa.edu.iq

https://doi.org/10.30572/2018/KJE/150301

ABSTRACT

In this research, thirteen specimens of reinforced concrete continuous deep beams were cast and tested. One was the main reference without openings, three were a reference for each style depending on the arrangement of the openings, while the other nine were strengthen beams using NSM technology. Three models were used to implement the strengthening (horizontal, vertical and inclined). The results showed an increase in load capacity after applying strengthening to the specimens, as well as an improvement in stiffness and ductility. The specimens with inclined strengthening gave the highest increase in load capacity The increase rates ranged between (19%-30%), The specimens with horizontal strengthening gave an increase ranging between (7%-26%), The specimens with vertical strengthening also gave an increase ranging between (7%-22%).

KEYWORDS

Strengthen, Near Surface Mounted, Deep Beam, Failer Mode, Crack Patterns.

1. INTRODUCTION

The need for strengthening and repair procedures for reinforced concrete structural elements in buildings and bridges has become necessary all over the world, and this confirms the importance of this aspect in the construction concrete industry. This led to the use of various technologies to serve these aspects, the most common of which are Near Surface Mounted NSM and Externally Bonded Reinforcement EBR, which have gained great acceptance in the global engineering community. The NSM technology involves inserting strips or bars into previously drilled grooves and then attaching them to them with an adhesive epoxy. NSM technology provides greater strength to the structure and makes it less susceptible to fire, failure, mechanical damage and premature aging. It also reveals better durability, stress sharing mechanisms and fatigue performance, as the reinforcement is located inside the structural member. However, the NSM method has some restrictions. The beam specimens to be strengthened must have sufficient width for the necessary edge clearance and clear spacing between the adjacent NSM grooves. (Hosen, et al., 2015). The NSM-FRP technology has been developed recently, as it involves placing FRP reinforcement inside pre-prepared grooves. NSM gives an increase in the flexural strength of concrete sills compared to external reinforcement of FRP. Also, reinforcement using NSM is less likely to separate from the concrete sill pillars. (Zhou, et al., 2013) Providing openings in the beams has become necessary due to the presence of corridors that must be taken into account when designing buildings to meet the needs of electrical and mechanical services and to become corridors through which (Yang & Ashour, 2008). According to the architectural need, the sizes and shapes of the openings are designed. The presence of openings in the beams causes non-linear stress along the length of the beam, and this leads to a different behavior from beams that do not contain openings. The presence of openings in the deep beams also leads to a reduction in the cross-sectional area of the beams, which reduces the strength and rigidity of the beam and leads to a deviation in the behavior of the deep beams. (Chin & Doh, 2015). In general, the definition of deep beams is the members that are loaded from one side and supported by the opposite side . This constitutes compression members that resemble beams between the loads and supports, and this must meet points a and b. (318, ACI Committee, 2019): (a) The clear distance between supports for deep beams should be less than four times the total length of the beams. (b) Loads must be concentrated in areas at a distance of less than two times the length of the beams from the faces of the supports. The common uses of deep beams are many, as they are usually used as members to distribute loads, as they are used in foundations in strips or slabs and marine structures shear wall structures that resist lateral forces, soil diaphragms, pile caps, building

walls. (Lafta, Y J; Ye, Kun, 2016) . The field of interest in structural engineering and building is concerned with reinforced concrete continuous deep beams (RCCDBs), as they have many common examples, including: Transfer girders, pile caps, tanks, folded frames, and foundation walls It carries a few loads and then distributes them to be supported from a few support points (Khalaf, et al., 2021) . Continuous deep beams and deep beams differ from shallow beams in that high moments are present and accompanied by strong shear zones in deep continuous beams, and failure occurs in these locations. While in deep beams, we find that high moments are offset by weak shear zones. Therefore, the mechanisms of failure in continuous deep beams differ from those in simple beams. The shear appears as a somewhat uniform diagonal compression in shallow beams, while it appears in the form of a connected arch or truss in deep beams. (Beshara et al., 2012).

1.1. Literature Review

There are several experimental studies that included the process of strengthening simple and continuous deep beams with or without openings.

In 2020 Al-Issawi & Kamonna tested thirteen deep beams with NSM-deformed steel bars under shear stress. Support plates were placed to prevent stress concentration. The tests included control and strengthened beams. Variables like bar spacings, diameters, and angles influenced performance. Results showed a 7.35-20.6% increase in ultimate capacity and improved ductility and diagonal crack width with more intensive strengthening schemes (Al-Issawi, A S and Kamonna, H H;, 2020). In 2020, Ramesh & Eswari tested six reinforced concrete beams, including a control beam, strengthened RC beam, and four GFRP strengthened RC beams. The study found that adding 1.5% of basalt and polyolefin fibers significantly improved the overall performance of the beams. The fiber volume fraction increased by 98.39 and 48.67% compared to the control beam and strengthened RC beam. The combination of basalt and polyolefin fibers also improved the interfacial contact between concrete surfaces and FRP laminates (Ramesh, B and Eswari, S, 2020). In 2020, Kamonna and Al-Khateeb conducted experimental research to strengthen the deep beams, their number was thirteen deep beams, and they used variables that included the size, shape of the openings and diameter of the steel bars. The type of loading was under the influence of four loading points. The results showed that the presence of openings reduced the final failure rate of the beam, so the square openings located in the loading area were 49. % for square openings located in the shear failure path area, it was 56%, while for rectangular openings, it increased by about 70%, while the use of reinforcement bars increased the bearing capacity, as the vertical bars increased by about 14%, while for

horizontal and vertical bars together, it increased by 40%, and when using bars in a diamond shape, it increased by 34%. The effect of the diameter of the skewers increased the loading capacity by 6%. (Kamonna & Al Khateeb, 2020). In 2021, Mansour & El-Maaddawy tested eight deep beams, adding NSM-CFRP reinforcement to strengthen six around cutouts. The NSM-CFRP systems fully recovered original shear strength, except for two cases where only 93% and 94% of capacity were restored. Finite element simulations were created to simulate nonlinear behavior, and the numerically predicted deflection response, CFRP strain response, and fracture forms were in good agreement with the testing results. (Mansour, M and El-Maaddawy , T, 2021). In 2022, Karimizadeh et al. conducted a study on eleven deep RC beams, constructing them uniformly and undergoing a three-point monotonic bending test. The beams were tested using steel plates of the same thickness to prevent plate failure. Welding two U-shaped bars to the loading plates reduced stress concentration. Results showed that specimens retorted by the SPF increased loading capacity and impact strength by 115% and 337%, respectively (Karimizadeh et al., 2022). In 2020, Al-Bdari et al. conducted a study on the impact of carbon fiber reinforced polymers (CFRP) on the structural behavior and shear resistance capacity of deep beams. They tested twelve continuous two-span beams, which were loaded with two-point loads and rested on steel supports. The study found that the hybrid technique increased the load carrying capacity of deep beams by up to 58.5% compared to beams without a strengthened control one (Al –Bdari et al., 2020). In 2021, Al-Bdari et al. conducted a study on seven reinforced SCC continuous deep beams after retrofitting with CFRP using three techniques: externally bonded reinforcing (EBR), near surface mounted technique (NSM), and a hybrid technique. The beams were tested with two symmetrical point loads and were subjected to shear failure tests. The results showed that applying EBR CFRP strips vertically increased loading capacity, while NSM CFRP rods placed horizontally showed higher ultimate load capacity and final deflection values. The study concluded that applying the hybrid technique is more effective (Anon., 2021). Khalaf et al's 2021 study tested the strength and stiffness of reinforced concrete continuous deep beams (RCCDBs) with large openings using carbon fiber reinforced polymer (CFRP) strips. The study found that large openings reduced ultimate load by 21% and 7% for un-reinforced and strengthened specimens, respectively. However, CFRP strips prevented further deterioration by increasing specimen capacity by 17% compared to un-strengthened ones. The research highlights the potential of CFRP strips in strengthening RCCDBs (Khalaf, et al., 2021).

This experimental research will include a strengthening process for reinforced concrete continuous deep beams with openings using NSM technology because of the necessity of this.

2. EXPERIMENTAL WORK

Thirteen continuous deep concrete beams were tested, one was the main reference for all, three had different openings, they were external, internal, external and internal together. As for the remaining nine, they were strengthened using three reinforcement patterns using NSM technology.

2.1. Details Of Specimens

All beams had a length of (2200 mm), with (150 mm) width and (500 mm) height as shown in Fig.1 A preliminary design using (strut and tie) model that described in (ACI-318.14) was conducted on control beam to find the main reinforcement. with shear span-to-overall depth ratio (a/h) equal to 1.0 and effective length to overall depth ratio (ln /h) equal 2.0, to ensure that the beams will behave as deep beams (ACI code). All beams were tested under two-point top loading. Four bars of Ø 16 mm were provided as bottom and top longitudinal reinforcement for each layer. The ends of all beams extended 100 mm beyond the support's centerlines and the steel bar had a 90º hook of length 180 mm at each end to provide sufficient anchorage. The concrete bottom cover of 25 mm and 50 mm as top cover were adopted to prevent splitting failure. All specimens were reinforced in bottom and top with two layers (4 Ø 16) bars for each as longitudinal reinforcement and three bars of (Ø 10) were used for linking longitudinal reinforcement see Fig.1. The tested beams were made without vertical and horizontal shear reinforcement to ensure the shear failure mode for the control specimens. The designed concrete compressive strength was (fc'= 28 MPa).

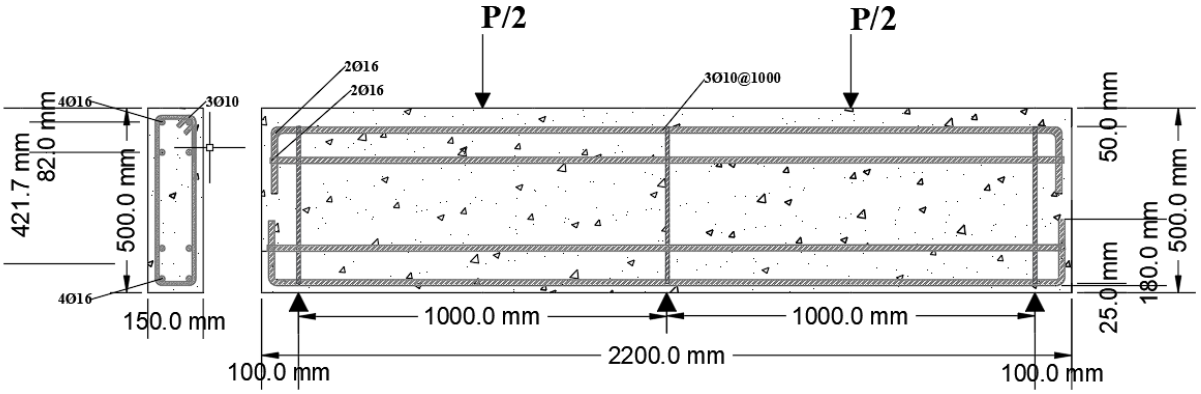

Fig. 1 Special details (dimensions, reinforcement) of the control beam

2.2. NSM Strengthened System

2.2.1. Details Of Group One

In this group, there were four square openings with equal spacing, and they were strengthened using horizontal, vertical and inclined reinforcing bars. As is clear in the Fig. 2.

2.2.2. Details of Group Two

In this group, there were two openings near to the end supports, and they were strengthened using horizontal, vertical and inclined reinforcing bars. As is clear in the Fig. 3.

2.2.3. Details of Group Two

In this group, there were two openings near to the middle support, and they were strengthened using horizontal, vertical and inclined reinforcing bars. As is clear in the Fig. 4.

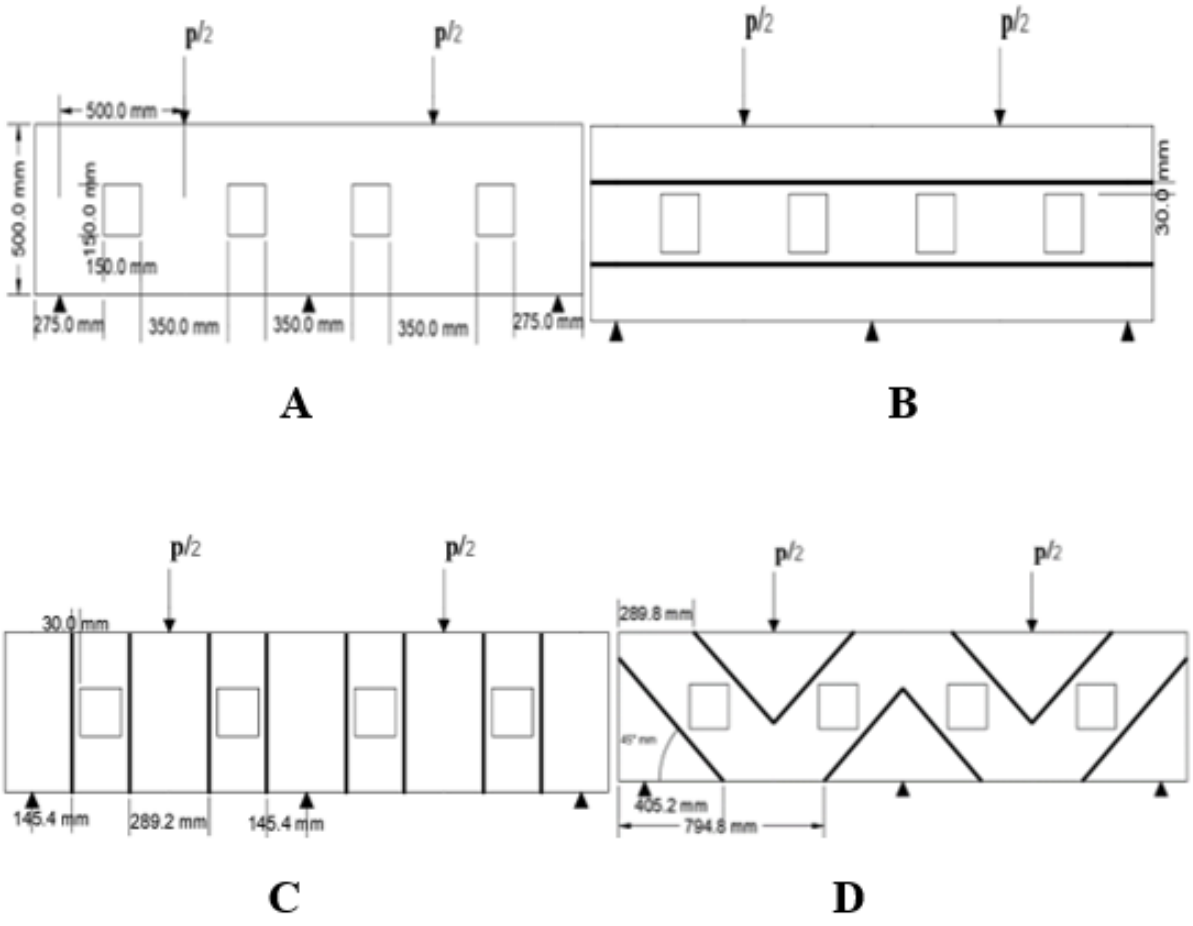

Fig. 2 General details of beams tested of group one

A: General details of the control beam for the first group, B: General details of the horizontal strengthening of the first group, C: General details of the vertical strengthening, D: General details of the inclined strengthening of the first group.

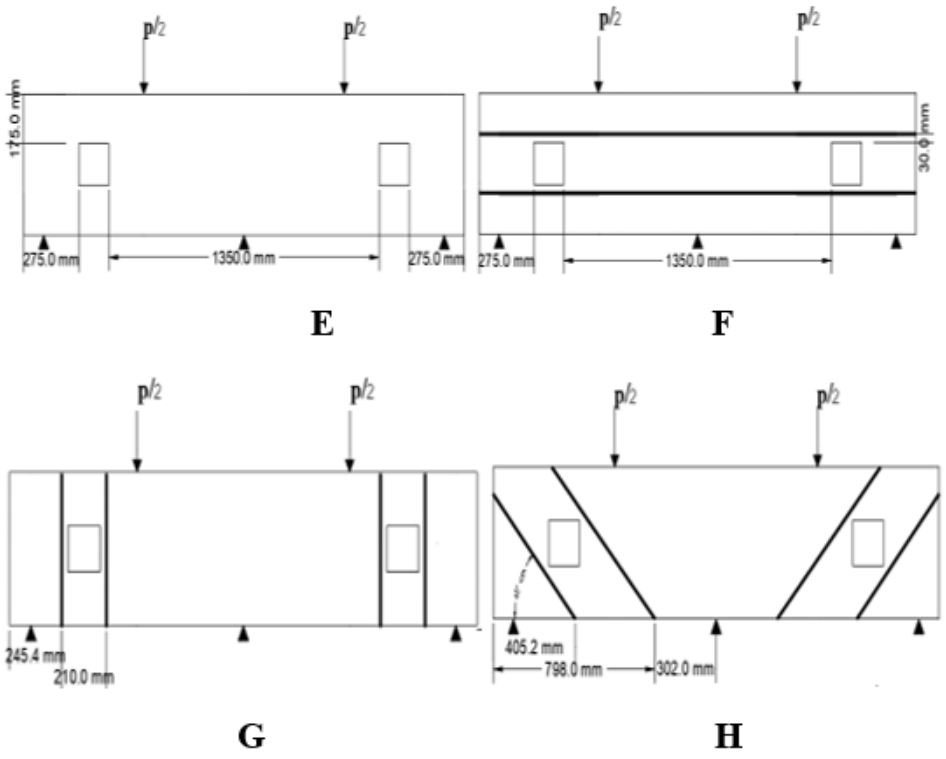

Fig. 3 General details of beams tested of group two

E: General details of the control beam for the second group, F: General details of the horizontal strengthening of the second group, G: General details of the vertical strengthening, H: General details of the inclined strengthening of the second group.

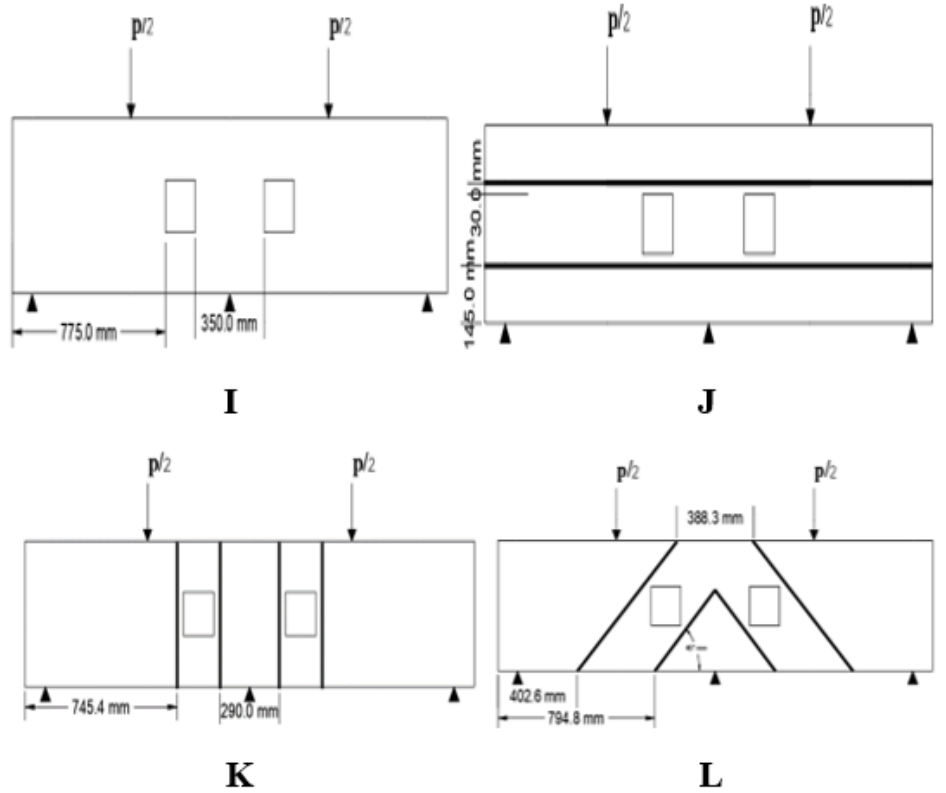

Fig. 4 General details of beams tested of group three

I: General details of the control beam for the first group, J: General details of the horizontal strengthening of the third group, K: General details of the vertical strengthening of the third group, L: General details of the inclined strengthening of the third group.

Table 1. Details of the tested continuous deep beams

Group Nu.	Specimen symbol	Explanation of the symbol
--------	CB	Control beam
Group one	CBSO4	Control beam-4square opening
	BSO4H	beam-4square opening- Horizontal strengthening
	BSO4V	beam-4square opening- Vertical strengthening
	BSO4I	beam-4square opening- Inclined strengthening
Group two	CBSEO2	Control beam-2External square opening
	BSEO2H	beam-2External square opening- Horizontal strengthening
	BSEO2V	beam-2External square opening- Vertical strengthening
	BSEO2I	beam-2External square opening- Inclined strengthening
Group three	CBSIO2	Control beam-2Internal square opening
	BSIO2H	Control beam-2Internal square opening- Horizontal strengthening
	BSIO2V	Control beam-2Internal square opening- Vertical strengthening
	BSIO2I	Control beam-2Internal square opening- Inclined strengthening

2.3. Materials Properties

The concrete mix components were supplied by (Asad Al-Najaf Ready Mix Concrete Company), Ordinary Portland cement was used, which was manufactured from the production of the Karbala Factory (Karbala / Iraq), the results were presented in Table 2 and Table 3 respectively. The clean water was used in mixing and curing the specimens. Fine aggregates were taken from the natural sand available in Bahr Al-Najaf quarries the results achieve the requirements of the specifications as shown in Table 4. The crushed gravel taken from the Nabaie area was used as coarse aggregate in the concrete mix, and the results achieve the requirements as shown in Table 5. Sikadur-30 manufactured by Sika company used to bond the strengthening bars with concrete in the grooves drilled with (NSM) technique the properties of the epoxy are obtained from the factory datasheet, as shown in Table 6. In this study, deformed steel reinforcement bars of Ukrainian origin were used the results were within the limits of the standard, as shown in Table 7.

Table 2. Chemical specifications for cement

Chemical compound	Test result	Iraqi Standard (IQ. S No .5/1984)
SiO2	21.1%	----------
Cao	63.3%	----------
Fe2O3	4.13%	
L.S. F	.95	Ranges (0.66-1.02% for Portland cement types except Low heat cement)
MgO	2.91%	Not more than 5%
SO3when C3A < than 5%	----------	Not more than 2.5%
SO3 when C3A > 5%	1.75%	Not more than 2.8%
Loss on Ignition	3.12%	Not more than 4%
Insoluble Residue	1%	Not more than 1.5%
C3S	40.72%	----------

Chemical compound	Test result	Iraqi Standard (IQ. S No .5/1984)
C2S	27.132%	----------
C3A	8.971	----------
C4AF	9.994%	----------
M.S	2.172	----------
M.A	1.967	----------
Free Lime	.713%	----------

Table 3. Physical specifications of cement

Physical property	Time minute	Limits of Iraqi Specification No.5/1984
Initial Setting time (Vicat minute)	65	Not less than 45 minutes
Final setting time (Vicat minute)	100	Not more than 600 minutes
Compressive strength in age(3days) N/mm2	30.45	Not less than 15N/mm2
Compressive strength in age(7days) N/mm2	27.97	Not less than 23N/mm2

Table 4. Results of sieve analysis of fine aggregate

Sieve size (mm)	Fine aggregate% (Passing)	Limit of IQS (45/1984), zone2
10	100	100
4.75	88	90-100
2.36	89	75-100
1.18	78	55-90
.6	56	35-59
.3	21	8-30
.15	9	0-10

Table 5. Sieve Analysis Results of Coarse Aggregate

Sieve size (mm)	Coarse aggregate % (Passing)	Limit of IQS (45/1984)
19	100	95-100
14	75	------
10	37	30-60
5	3	0-10

Table 6. Specifications for epoxy adhesive

Appearance	Component (A): white, Component(B): black Component (A+B): gray
Mixing ratio (A: B)	3:1
Modulus of elasticity	10000 N/mm^2
Compressive strength	>85 N/mm^2
Tensile strength	>17 N/mm^2
Shear strength	≈7 N/mm^2
Tensile Adhesion strength	For concrete >4 N/mm^2, For steel >22N/mm^2

Table 7. Results of the tensile strength test of steel bars

Diameter Bar (mm)	Yield strength Fy (N/mm^2)	Tensile strength (N/mm^2)	Elongation %	Limit according ASTM A615M-05a		
				fy (N/mm^2)	Tensile strength (N/mm^2)	Elongation %
16 mm	530	720	14.8%	420	620	12
10 mm	515	678	11.985%	420	620	12

2.4. Concrete Mix

The proportions of the concrete used are shown in the Table 8.

Table 8. Concrete Mix

Material	Cement (kg/m^3)	Coarse Aggregate (kg/m^3)	Fine Aggregate (kg/m^3)	Water (l/m^3)	w/c
Amount	336	1130	683	155	.4

2.5. properties Of Hardened Concrete

2.5.1. Compressive Strength

Six cubes with dimensions of 150 mm were tested to determine the compressive strength of the specimens. Three of them were tested at age 28 days and the other three were tested at test time of the beams. The compressive strength of the concrete was adopted as the average for the last three cubes strength, as shown in Table 9.

2.5.2. Tensile Strength

The tensile strength of concrete was obtained by testing the split tensile for three cylinders with dimensions of 300 mm in length and 150 mm in diameter at 28 days, as shown in Table 9.

Table 9. Compressive and split tensile Concrete Strengths

Specimen	time	compressive strength N/mm^2	tensile strength N/mm^2
1	At Test Time	33.8	3.7
2		31.1	3.1
3		32.6	2.89
Average		32.5	3.23

2.6. Test Setup and Instrument

2.6.1. Testing Process

The examination process for the beams was carried out in the construction laboratory at the University of Kufa, College of Engineering.

Use hydraulic device with capacity of 2000 KN. The distances were arranged in proportion to the dimensions of the designed beams. To avoid concrete failure at the loading and support points, rubber sheets were placed.

Recording the results: The loading results were recorded with a variation of 10 kN, and the deflection and crack width were calculated every 100 KN until failure.

2.6.2. Test Instrument

2.6.2.1. Deflection Measurement

The mid-span deflections were measured with a dial gauge has 0.01mm/div. sensitivity, as shown in Fig.5.

Fig. 3 Dial Gauge Device

2.6.2.2. Crack Meter and Vernia

Crack meter was used to measure crack width up to 0.5mm. When the crack widths exceed 0.5mm the Vernia was used to measure the width of the crack. Crack meter and Vernia are shown in Fig. 6.

Fig. 4 Crack meter and Vernia

2.7. Preparation of Specimens

The frameworks were washed and oiled after that Reinforcing steel were put in the frameworks carefully, the concrete was casted into the frameworks in three layers. Each layer was compacted by using mechanical vibrators, six cubes and three cylinders were casted. The cubes were casted in three layers and each layer was compacted using 36 blows by steel bar. The cubes and cylinders were used to determine compressive and tensile strength respectively. Three days later, the frameworks were removed and the samples were covered with wet burlap and the curing period continued up to 28 days.

2.8. Strengthening Process by NSM Bar Technique

The boundaries of the grooves required for placement of NSM reinforcing bars are determined. The first step was to locate the reinforcement and mark it with a pen to make drilling and carving easier. The second step was to drill both sides of the threshold, front and back, with a diamond-blade concrete saw. The third step is to apply epoxy adhesive to half the depth of the groove, then place the steel skewer, then fill the groove. With epoxy to cover it completely. After that, it is left for eight days to be suitable for examination according to special instructions. To distinguish the reinforcement areas, they were painted red, and the beams were painted white to facilitate identification of crack areas during testing.

3. RESULTS AND DISCUSSION

3.1. Cracks Patterns and Failure Mode

Table 10 presents the experimental results for all tested specimens.

3.1.1. Control Beams

The specimen CB serves as a reference for other control specimens. No sudden changes in strength occurred throughout the loading history until sudden shear failure occurred. Cracks propagated uniformly in the two-sided beam, starting with flexural cracks at 60 KN, increasing to shear cracks at 44% of maximum load, and finally reaching failure at 570 KN. Fig. 7-A shows the pattern and path of cracking.

While the reference specimens for the first group is CBSO4 (The spaceman's beam had four square openings), causing stresses to concentrate in their corners, leading to a first shear crack. Flexural cracks appeared at 70 KN load, extending vertically until 300 KN. Shear cracks appeared near supports and extended diagonally. When loading reached 340 KN, the beam failed, resulting in diagonal shear failure and bending failure. Fig. 7-B shows the pattern and path of cracking.

As for the control beam for the second group, CBSEO2, the study found that flexural failure in the deep continuous beam began at a load of 70 KN, while diagonal shear failure developed at a load of 90 KN. The failure continued to develop as the device load increased up

To 470 knots, causing a drop of 21.276%. Fig. 7-AC shows the pattern and path of cracking.

The control beam of the third CBSIO2 group showed a 14% reduction in cracks compared to the reference beam. The cracks started at the loading point and gradually increased, eventually leading to radial shear cracks. The threshold failed at a load of 500 nodes, an increase of 7.276% compared to the second set. This was because the openings were far from the failure path. Fig. 7-D shows the pattern and path of cracking.

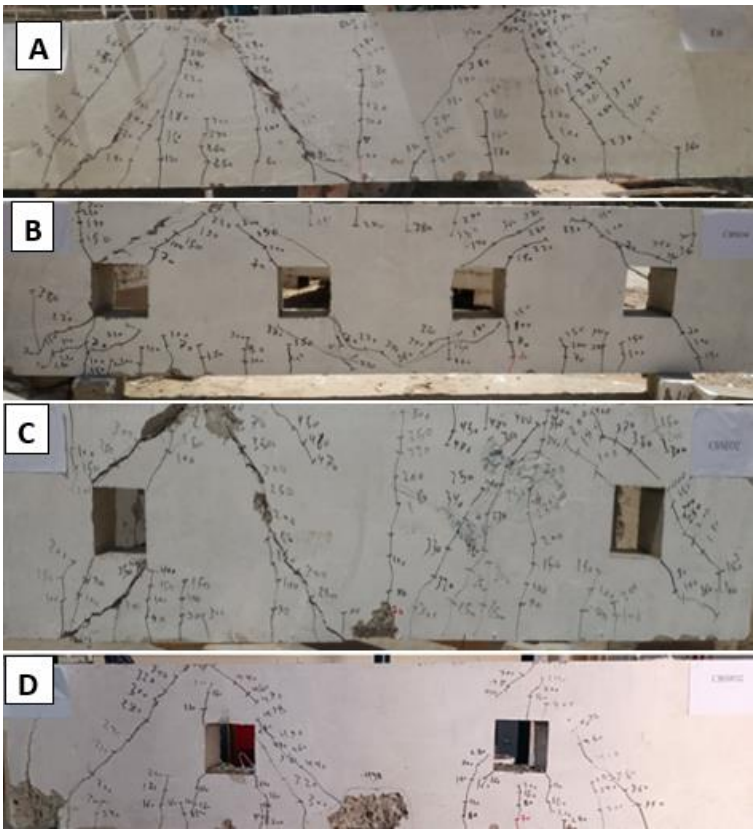

Fig. 5 Crack pattern of control beams

3.1.2. Strengthened Beams with Vertical Type

The specimen BSO4V was strengthened with (8) vertical bars on both beam faces to improve tensile and shear strength. This configuration increased capacity compared to the control beam, as the added steel resisted most loading before failure. The first crack started near the beam face at 70 KN, and more cracks propagated and spread within the shear span. The high shear resistance provided by the NSM steel bars restricted diagonal shear failure, improving the ultimate load by 7.894%. The failure pattern showed a displacement to the other edge of the opening. The crack patterns and failure mode of specimen BSIO2V are shown in Fig. 8-E.

The use of vertical reinforcement bars to strengthen the sample BSEO2V increased the failure tolerance by 10.638% compared to the reference. The vertical reinforcement in the first group increased by 2.744%. Bending failure began at a loading point of (90 KN) and then gradually increased. Diagonal shear failure began at loading (110 KN) but stopped due to minor impacts. The failure path was slightly skewed, resulting in sustained beam failure at (520 KN). The crack patterns and failure mode of specimen BSIO2V are shown in Fig. 8-F.

vertical reinforcing bars used to strengthen the continuous beam (BSIO2V), which led to an increase in the maximum failure load by 22% over the reference and 11.362% over the previous vertical reinforcement. This is due to the long failure path, which is shear failure, as the openings are farther from the area with the greatest stresses, which causes a delay in the appearance of the crack and an increase in the load. The radial shear stresses started to increase at loading (150 KN) and deviated slightly at loading (180 KN). The vertical bars prevented this deflection, limiting failure. Overloading the device resulted in failure at load (610 KN). The crack patterns and failure mode of specimen BSIO2V are shown in Fig. 8-G.

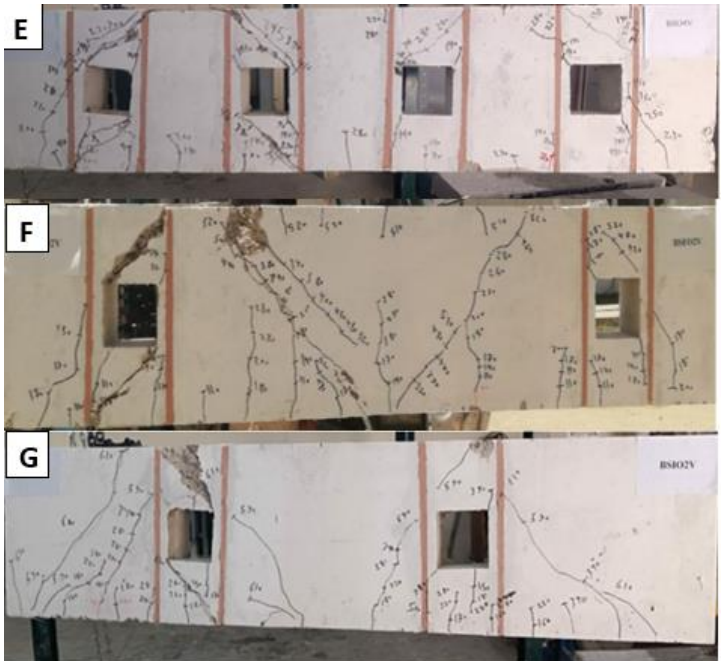

Fig. 6 Crack pattern of beams with vertical reinforcement

3.1.3. Strengthened beams with horizontal type

The specimen BSO4H was strengthened with horizontal bars on both beam faces, resulting in an enhancement in ultimate load of 7.894% compared to the unstrengthen specimen and a decrease of 50% compared to the CB. Cracks began at the opposite corners of the opening and bottom face below the opening at a load of (90 KN), indicating an increase in initial failure load. The failure form deviated from the reference failure, indicating that horizontal reinforcing bars changed the path of failure and became a good barrier. The vertical type of strengthening also showed the same failure load, but the acute angle formed with the diagonal failure line was identical to both horizontal and vertical bars. Crack patterns and failure mode for specimen BSO4V are shown in Fig. 9-H.

The study used horizontal reinforcing bars to reinforce a beam BSEO2H, resulting in a 12.765% increase in loading compared to the reference maximum loading. This increase was

4.871% higher than the horizontal reinforcement of the first group, compared to 26.316% for the reference maximum load. Diagonal shear failure appeared at the loading point (200 KN) in the middle of the continuous deep beam and increased with increasing loading. Bending failure began from the top of the center of the beam at (280 KN) loading and continued diagonal shear failure to the extent of complete failure at (530 KN) loading. The failure path deviated from its path, suggesting that the reinforcing bars formed a good horizontal barrier, especially at the ends. Crack patterns and failure mode for specimen BSEO2H are shown in Fig 9-I.

The use of horizontal reinforcing bars in a specimens BSIO2H resulted in a 26% increase in maximum load, compared to the previous horizontal reinforcement by 13.235%. This increase was attributed to the shorter shear failure path due to the distance of square openings from the area of greatest stresses of the continuous beam. Bending cracks appeared at (90 KN) load, stopped at (300 KN), and at (220 KN) load, diagonal shear stresses appeared from the right side of the specimen from the bottom and developed upwards until the failure at (630 KN). The reinforcement helped change the path of failure, slightly deviating from its position relative to the reference failure shape, resulting in a slight increase in maximum failure load. Crack patterns and failure mode for specimen BSIO2H are shown in Fig 9-J.

Fig. 7 Crack pattern for beams with horizontal reinforcement

3.1.4. Strengthened beams with inclined type

The use of inclined reinforcement bars to strengthen a continuous deep beam BSO4I, increased the load by 23.684% while reducing the maximum load by 50%. The increase was more pronounced than horizontal and vertical, due to the larger acute angle formed with the diagonal shear failure line. The first failure occurred at the bearing (70 KN), a bending failure

in the middle of the continuous deep sill, and it stopped rising to mid-height. Diagonal shear failure began at load (180 KN). The failure mode was significantly skewed, indicating that the inclined reinforcing bars presented the best ratio, as they were opposite to the inclination of the diagonal shear failure line and formed the highest acute angle. The specimen failed at a load of (470 KN). The crack patterns and failure mode of specimen BSO4I are shown in Fig.10-K.

The use of BSEO2I beam inclined reinforcement bars resulted in the highest increase in maximum load, reaching 19.148%. This type of reinforcement was the best compared to horizontal and vertical reinforcement. Bending failure started at a load of (150 KN) and then gradually increased, while diagonal shear failure started at a load of (280 KN). The failure path deviated to the adjacent edge, indicating that the rails changed path. The reference failure was continuous with the diagonal lines but was interrupted in the reinforcement region and varied until failure occurred at the bearing (560 KN). This type showed the best increase, similar to the previous group. The crack patterns and failure mode of specimen BSEO2I are shown in Fig.10-L.

Specimen BSIO2I used diagonal reinforcement bars, which were found to be the best choice due to their opposite path to diagonal shear failure. This prevents crack development and increases the maximum failure load by approximately 30% compared to the reference specimen. Curved cracks appeared at the load (170 KN), continued until the load (350 KN), and stopped in the middle of the sample. At load (200 KN), radial shear cracks started near the loading points and regularly on both sides. The failure path was deviated away from the bar,

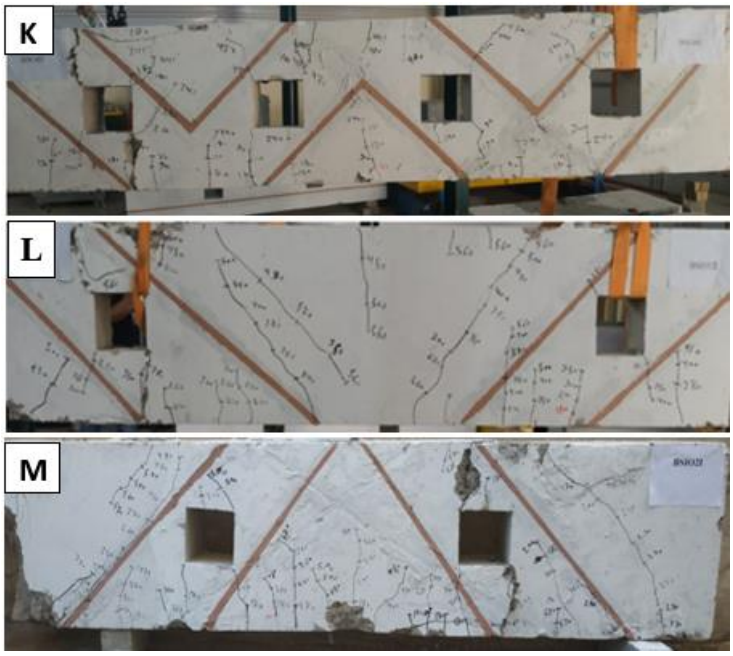

Fig. 8 Crack pattern for beams with inclined reinforcement

creating a barrier that strongly prevented the development of radial shear cracks until the beam failed at load (650 KN). The crack patterns and failure mode of specimen BSIO2I are shown in Fig.10-M.

Table 10. Test Result of all group

Group	Beam name	Ultimate load (kn)	Changed in ultimate load (%)	Deflection At failure (mm)	Failure modes
--------	CB	570	----------	4.41	Shear
Group one	CBSO4	380	50	3.1	Shear
	BSO4H	410	7.894	3.25	Shear & Flexural
	BSO4V	410	7.894	3.27	Shear
	BSO4I	470	23.684	4.26	Shear & Flexural
Group two	CBSEO2	470	21.276	4.62	Shear & Flexural
	BSEO2H	530	12.765	3.47	Flexural
	BSEO2V	520	10.638	3.23	Shear & Flexural
	BSEO2I	560	19.148	1.82	Shear & Flexural
Group three	CBSIO2	500	14	3.62	Shear & Flexural
	BSIO2H	630	26	2.24	Shear
	BSIO2V	610	22	2.49	Shear
	BSIO2I	650	30	1.84	Shear & Flexural

3.2. Load Deformation Curve

3.2.1. Control Specimens

Fig. 11 shows the behavior of the deformation load curves for the controlling beams. The curves started with a linear behavior and then turned into a curve. The controlling beam CB is above of the other curves as it is higher in load capacity, followed by the two specimens CBSIO2, CBSEO2, then the CBSO4. This is due to the increase in openings, as the higher the capacity, the lower the bearing capacity.

3.2.2. Group One

The application of NSM technology led to a clear improvement in the load capacity of the strengthening beam, and Fig. 12 shows the increase in the load of the strengthening beams as the curves increased above the curve of the controlling beam CBSO4. We also notice that the BSO4I curve showed the best increase.

3.2.3. Group Two

The deformation load curves for the beams after strengthening showed an improvement in the physical properties of the beam relative to the reference beam, as the load capacity increased for all types used, and BSEO2I showed the highest increase in bearing capacity, followed by the two beams BSEO2H and BSEO2V, and the hardness also improved.as shown in Fig. 13.

3.2.4. Group Three

The curves BSIO2I, BSIO2H, BSIO2V are higher than the reference curve CBSIO2, and this means that after strengthening, the properties of load capacity, ductility and hardness improved.as shown in Fig.14.

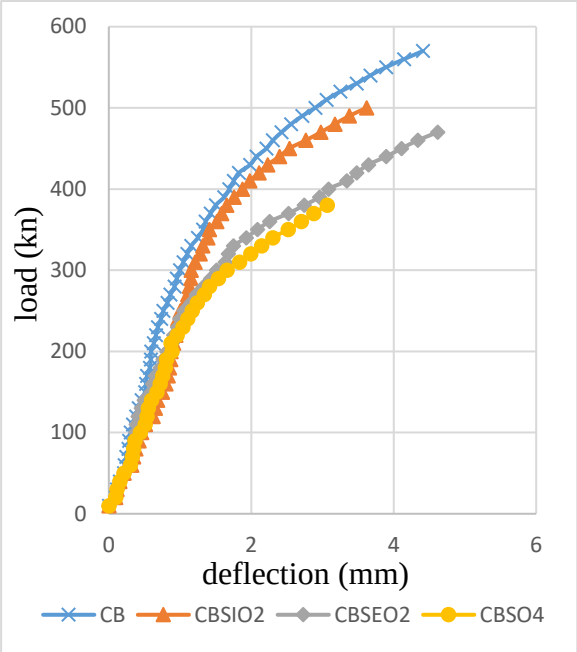

Fig. 9 Load-deformation curves for control beams

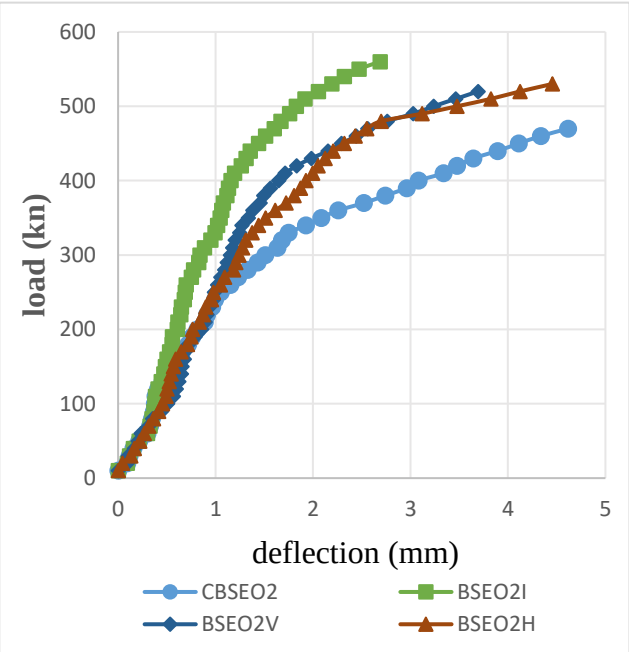

Fig. 10 Load-deformation curves for beams of the first group

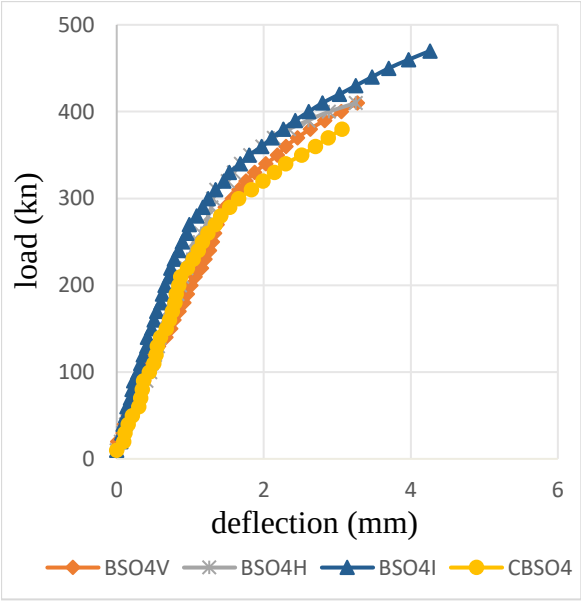

Fig. 11 . Load-deformation curves for the beams of the second group

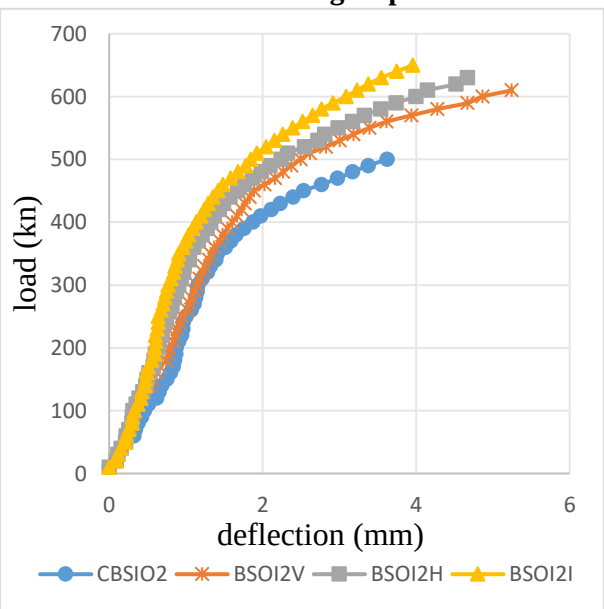

Fig. 12 Load-deformation curves for the for beams of the third group

4. CONCLUSION

The use of NSM technology for the purposes of strengthening continuous deep beams with openings in this experimental research led to reaching certain results, which are as shown in the points below:

1. The presence of openings led to a reduction in the bearing capacity of the beams by certain percentages.
2. The load-deformation curve shows that it began in a linear manner and then gradually transformed into curves. We find that the curves for beams with openings are below the curve for the main controlling beam, meaning that they are less durable.
3. After applying NSM technology, the bearing capacity increased from (7.894%-30%).
4. the load-deformation curves for beams strengthened using NSM technology above the curves before the strengthening process, this means an increase in bearing capacity, and their physical properties also improved, such as ductility and stiffness.
5. After applying the NSM technique, the vertical and horizontal reinforcement bars gave somewhat similar percentages of increase in bearing capacity because the angle formed between the diagonal shear failure line and the strengthening bars is close.
6. After applying the NSM technique, the inclined reinforcement bars gave the highest increase in bearing capacity, which was 30%. This is due to the fact that the angle between the inclined bars and the diagonal shear failure line was larger than the vertical and horizontal bars.

5. REFERENCES

Chin, S. C., & Doh, S. I. (2015). Behaviour of reinforced concrete deep beams with openings in the shear zones. Journal of Engineering and Technology (JET), 6(1), pp.60-71.

318 ,ACI Committee, 2019. Building Code Requirements for Structural Concrete (ACI 318-19). Farmington Hills: American Concrete Institute.

Al-Bdari, W. J., Al-Bayati, N., & Al-Shaarbaf, A. S. (2020, February). Structural behaviour of SCC continuous deep beam strengthened with carbon fiber NSM and hybrid techniques. In IOP Conference Series: Materials Science and Engineering (Vol. 737, No. 1, p. 012026). IOP Publishing.

Al-Issawi, A. S. H., & Kamonna, H. H. (2020). Experimental study of RC deep beams strengthened by NSM steel bars. Materials Today: Proceedings, 20, 540-547.

Al-Bdari, W. J., Al-Bayati, N. A., & Al-Shaarbaf, I. A. (2021). Structural Behavior of Retrofitted Reinforced SCC Continuous Deep Beam With CFRP and Hybrid Techniques. Engineering and Technology Journal, 39(7), 1153-1163.

Beshara, Fouad B.A.; Shaaban, Ibrahim G.; Mustafa, Tarek S., 2012. Behavior of Reinforced Concrete Continuous Deep Beams in Shear. Engineering Research Journal, 10 Jul, Volume 17.

Hosen, M. A., Jumaat, M. Z., & Islam, A. S. (2015). Side Near Surface Mounted (SNSM) technique for flexural enhancement of RC beams. Materials & Design, 83, pp.587-597.

Kamonna, H. H., & Alkhateeb, L. R. (2020). Strengthening of reinforced concrete deep beams with openings by near surface mounted steel bar. Journal of Engineering Science and Technology, 15(4), pp.2559-2579.

Karimizadeh, H., Arabzadeh, A., Eftekhar, M. R., & Amani Dashlejeh, A. (2022). Shear Strengthening of RC Deep Beams with Symmetrically or Asymmetrically Positioned Square Openings Using CFRP Composites and Steel Protective Frames. Advances in Civil Engineering, 2022(1), 5352330.

Khalaf, M. R., Al-Ahmed, A. H. A., Allawi, A. A., & El-Zohairy, A. (2021). Strengthening of continuous reinforced concrete deep beams with large openings using CFRP strips. Materials, 14(11), 3119.

Lafta, Y. J., & Ye, K. (2016). Specification of deep beams affect the shear strength capacity. Civil and Environmental Research, 8(2), 56-68.

Mansour, M., & El-Maaddawy, T. (2021). Testing and modeling of deep beams strengthened with NSM-CFRP reinforcement around cutouts. Case Studies in Construction Materials, 15, e00670.

Ramesh, B., & Eswari, S. (2020). Structural response of GFRP strengthened hybrid fibre reinforced concrete beams. Materials Today: Proceedings, 33, pp. 463-469.

Yang, K.H. and Ashour, A.F. (2008) Effectiveness of Web Reinforcement around Openings in Continuous Concrete Deep Beams. ACI Structural Journal, Vol. 105, No. 4, pp. 414-424.

Zhou, Y., Gou, M., Zhang, F., Zhang, S., & Wang, D. (2013). Reinforced concrete beams strengthened with carbon fiber reinforced polymer by friction hybrid bond technique: Experimental investigation. Materials & Design, 50, pp. 130-139.